ACS APPLIED MATERIALS & INTERFACES

Research Article

www.acsami.org

Enhanced Tolerance to Stretch-Induced Performance Degradation of Stretchable MnO_2-Based Supercapacitors

Yan Huang,[†] Yang Huang,[†] Wenjun Meng,[†] Minshen Zhu,[†] Hongtao Xue,[†,‡] Chun-Sing Lee,[†,‡,§] and Chunyi Zhi*[,†,§]

[†]Department of Physics and Materials Science, and [‡]Center of Super-Diamond and Advanced Films (COSDAF), City University of Hong Kong, 83 Tat Chee Avenue, Kowloon Tong, Hong Kong, China

[§]Shenzhen Research Institute, City University of Hong Kong, Shenzhen, China

Supporting Information

ABSTRACT: The performance of many stretchable electronics, such as energy storage devices and strain sensors, is highly limited by the structural breakdown arising from the stretch imposed. In this article, we focus on a detailed study on materials matching between functional materials and their conductive substrate, as well as enhancement of the tolerance to stretch-induced performance degradation of stretchable supercapacitors, which are essential for the design of a stretchable device. It is revealed that, being widely utilized as the electrode material of the stretchable supercapacitor, metal oxides such as MnO_2 nanosheets have serious strain-induced performance degradation due to their rigid structure. In comparison, with conducting polymers like a polypyrrole (PPy) film as the electrochemically active material, the performance of stretchable supercapacitors can be well preserved under strain. Therefore, a smart design is to combine PPy with MnO_2 nanosheets to achieve enhanced tolerance to strain-induced performance degradation of MnO_2-based supercapacitors, which is realized by fabricating an electrode of PPy-penetrated MnO_2 nanosheets. The composite electrodes exhibit a remarkable enhanced tolerance to strain-induced performance degradation with well-preserved performance over 93% under strain. The detailed morphology and electrochemical impedance variations are investigated for the mechanism analyses. Our work presents a systematic investigation on the selection and matching of electrode materials for stretchable supercapacitors to achieve high performance and great tolerance to strain, which may guide the selection of functional materials and their substrate materials for the next-generation of stretchable electronics.

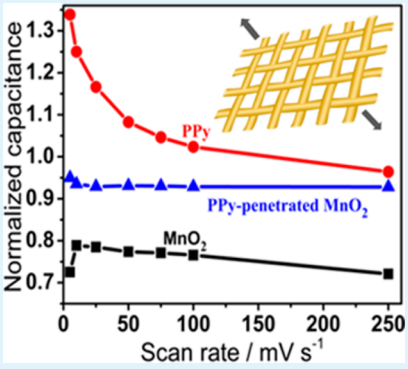

KEYWORDS: *stretchable supercapacitors, MnO_2 nanosheets, polypyrrole film, stretch-induced performance degradation, tolerance enhancement*

1. INTRODUCTION

The design of stretchable electronics[1−5] which can maintain great performance under stretch is essential for making their unprecedented applications practical such as future smart clothes,[6] epidermal electronics,[7] and electronic "eyeball" digital cameras, etc.[8] Electrodes of stretchable electronics are usually designed to be active materials coated on conductive stretchable substrates. However, the maximum sustainable strains for most electroactive materials are too limited (e.g., <1% for inorganic materials and metals and <5% for conductive polymers)[9] to sustain a significant strain deformation for stretchable substrates. Within the composite structured electrodes, the deformation mismatch between electroactive materials and substrates affects their morphologies and interfaces, which generates crucial influences on the performance of stretchable devices. Therefore, cracks always appear on active materials under stretch, resulting in an increase of resistance and greatly jeopardizing the performance.[10−14] However, no studies have been conducted to improve the degraded performance under stretch.[15,16] Thus, it is of primary importance to study how to enhance the stretch-induced performance degradation since it will determine the performance sustainability and guide the design of stretchable electronics.

In this article, we present a detailed study on effects of functional/substrate electrode materials matching the performance of stretchable supercapacitors under strain. As expected, being the electrochemically active electrode material, the conducting polymer PPy provides a great tolerance to strain due to its intrinsic ductility and perfect matching with the conductive mesh. On the contrary, the rigid structure of metal oxides such as MnO_2 nanosheets, induces dramatic supercapacitor performance degradation under strain, which is verified by detailed morphology and impedance analyses. Subsequently, an electrode of MnO_2 nanosheets penetrated by PPy is designed, and it is revealed that the PPy penetration can effectively enhance the tolerance to the stretch-induced

Received: October 31, 2014
Accepted: January 8, 2015
Published: January 8, 2015

DOI: 10.1021/am507588p
ACS Appl. Mater. Interfaces 2015, 7, 2569−2574

performance degradation observed in MnO_2 nanosheet electrodes, due to the intrinsically flexible PPy serving as a stress buffer. Our study indicates that for stretchable supercapacitors, the combination of conducting polymers and metal oxides may be the ultimate solution to achieve high performance and remarkable tolerance to stretch.

2. EXPERIMENTAL SECTION

2.1. Electrodeposition of the PPy Film and MnO_2 Nanosheets. Stretchable conductive filter meshes (200 mesh woven from 50 μm wires) with a width of 0.5 cm were washed in acetone, ethanol, and deionized water, and then used as substrates.

For the PPy-film supercapacitor, anodic electrodeposition of the PPy film was conducted for 1 min at a constant current density of 0.33 mA/cm^2 in a solution of 0.1 M *p*-toluenesulfonate acid, 0.3 M sodium *p*-toluenesulfonate, and 0.5% distilled pyrrole monomer (v: (v) at 0 °C.

For the MnO_2-nanosheet supercapacitor, MnO_2 nnaosheets were prepared by electrodeposition at 0.92 V vs Ag/AgCl for 15 min in a solution of 0.02 M manganese nitrate and 0.01 M sodium nitrate. As MnO_2 is susceptible to acid,[17,18] a very thin PPy film was electrodeposited on the as-grown MnO_2 nanosheets at 0.6 V vs Ag/AgCl for 0.5 min in order to provide some protection against the acid corrosion and not affect the MnO_2's intrinsic performance response to stretch.

For the PPy-penetrated MnO_2 supercapacitor, the same MnO_2 electrodeposition was followed by PPy electrodeposition at 0.8 V vs Ag/AgCl for 0.5 min. It should be noted that the mass of PPy obtained at 0.8 V vs Ag/AgCl is much more (over 14-fold) than the aforementioned PPy at 0.6 V vs Ag/AgCl (see Figure S1a, Supporting Information, showing the current during PPy electrodeposition at the former potential is much higher than the one at the later potential). Thus, the PPy's at 0.8 V vs Ag/AgCl are thick enough to modify the composite electrode's performance response to stretch, while the PPy at 0.6 V vs Ag/AgCl is so little that the typical performance response to stretch of MnO_2 can be mostly maintained in the MnO_2 supercapacitor as described below (Figure S1b and c, Supporting Information).

2.2. Fabrication of Solid-State Supercapacitors. Two identical as-grown samples were assembled together with a gel electrolyte of H_3PO_4 and PVA (electrolyte composition: 6 g H_3PO_4, 6 g PVA, and 60 mL deionized water). After gel solidification at room temperature, the solid-state supercapacitor was obtained with the electrolyte also serving as a separator.

2.3. Characterization. The microstructure and morphology of electrodes were characterized by scanning electron microscope (SEM, JEOL JSM-6335F) with an acceleration voltage of 5 kV and transmission electron microscope (Philips CM 20) with energy-dispersive X-ray spectroscopy (EDX). X-ray diffraction studies were performed on a Philips X'Pert High Resolution Materials Research Diffractometer using Cu Kα radiation (λ = 1.54 Å). Raman spectroscopy was obtained by a RENISHAW Raman microscope with an excitation wavelength of 633 nm. Cyclic voltammograms (CV) and galvanostatic charge−discharge (CD) measurements were performed on an electrochemical station (CHI 760E). Electrochemical impedance spectra (EIS) was measured at frequencies ranging from 0.01 to 100000 Hz with a potential amplitude of 5 mV. Supercapacitors were mounted onto two clips and stretched horizontally by a test bench (AMH-500, Yiding Co., Wenzhou).

3. RESULTS AND DISCUSSION

Stretchable supercapacitors are chosen as a typical example of stretchable electronics and PPy and MnO_2 as reprehensive electrochemically active materials for supercapacitors. On the one hand, supercapacitors are an important category of energy storage technologies in the development of sustainable energy, due to their high power density, fast rate of charge−discharge, and long cycling life, etc.[19−23] On the other hand, conducting polymers such as PPy and transition metal oxides such as MnO_2 are two types of very popular materials for supercapacitors.[24−29] They both store charges via fast and reversible redox reactions.[30−32] As a polymer, PPy exhibits intrinsic flexibility, while as a metal oxide, MnO_2 possesses a rigid structure.

A simply designed stretchable supercapacitor was fabricated to investigate materials matching among the conductive substrate, electrochemically active materials, and the electrolyte. It was found that stainless steel filter meshes woven by a plain weave technique could become very stretchable up to a strain of 40% when being tailored along a direction of 45° to its weft or the warp. This provides a facile and low-cost method to fabricate stretchable electronic devices without resorting to complicated treatments to obtain conductive and stretchable substrates. Figure 1a schematically shows the typical stretchable mesh structures used in this article. MnO_2 nanosheets and PPy films are electrodeposited onto the mesh substrate, separately, for the comparison of their performances under stretch (Figure 1b,c). Besides, PPy-penetrated MnO_2 is also prepared by the sequential electrodeposition of MnO_2 nanosheets and PPy onto the substrate (Figure 1d).

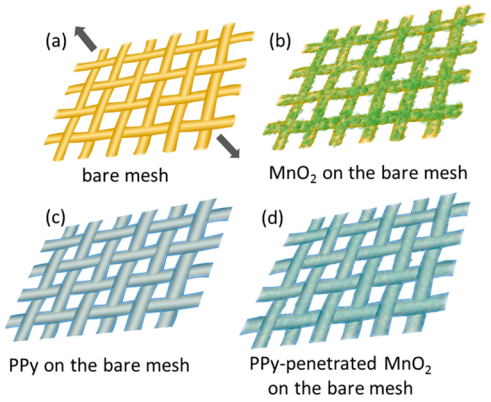

Figure 1. Schematic illustrations of fabricated electrodes: (a) tailored stretchable mesh (stress is along the direction of arrows). (b) MnO_2 nanosheet electrodeposited mesh. (c) PPy film electrodeposited mesh. (d) PPy-penetrated MnO_2 electrodeposited mesh.

SEM images of electrodes show clearly the two-dimensional hierarchical structure with MnO_2 nanosheets (Figure 2a−c) and PPy films (Figure 2d−f) uniformly electrodeposited onto the conductive mesh, including the areas of the cross-intersections. However, high magnification images show that the microstructures of MnO_2 nanosheets and PPy film are much different. The surface of MnO_2 is noncontinuous and has a flowerlike assembly structure of nanosheets (Figure 2b,c), while PPy forms a continuous film on the mesh (Figure 2e,f). For an X-ray diffraction (XRD) pattern collection, MnO_2 nanosheets are deposited on a fluorine-doped indium tin oxide (FTO) coated glass plate with the same electrodeposition conditions. Although the peaks of FTO are very strong (Figure 2g), typical peaks of MnO_2 are still notable showing the ε phase. Figure 2h presents the Raman spectrum of the polymer film electrodeposited on the mesh substrate, which confirms the species of as-synthesized PPy. The band at 622 cm^{-1} (peak a) is attributed to the ring torsion. The region at 684 cm^{-1} (peak b) corresponds to C−H wagging. The peak at around 930 cm^{-1} (peak c) corresponds to ring deformation. The band at 967 cm^{-1} (peak d) is attributed to the ring deformation

DOI: 10.1021/am507588p
ACS Appl. Mater. Interfaces 2015, 7, 2569−2574

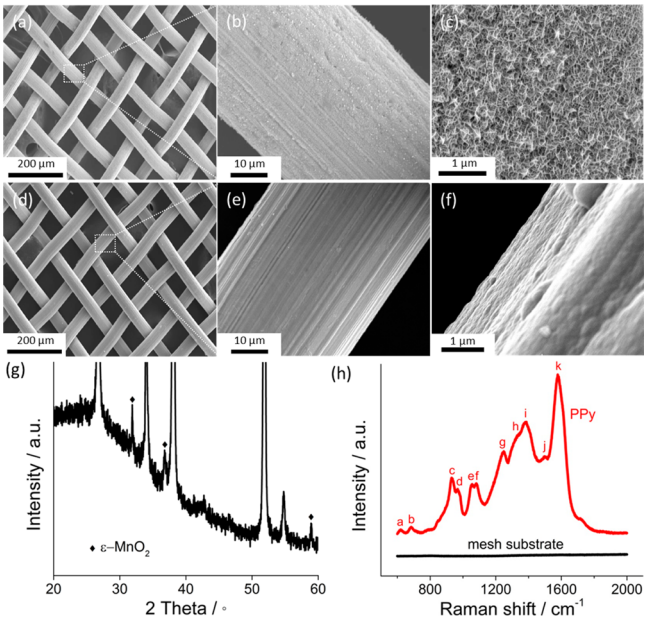

Figure 2. SEM images of the fabricated electrodes: (a–c) different magnifications of MnO_2 nanosheets. (d–f) Different magnifications of the PPy film. (g) XRD of the as-synthesized MnO_2 nanosheets showing the species of ε-MnO_2. (h) Raman spectrum of the as-synthesized material showing the species of PPy.

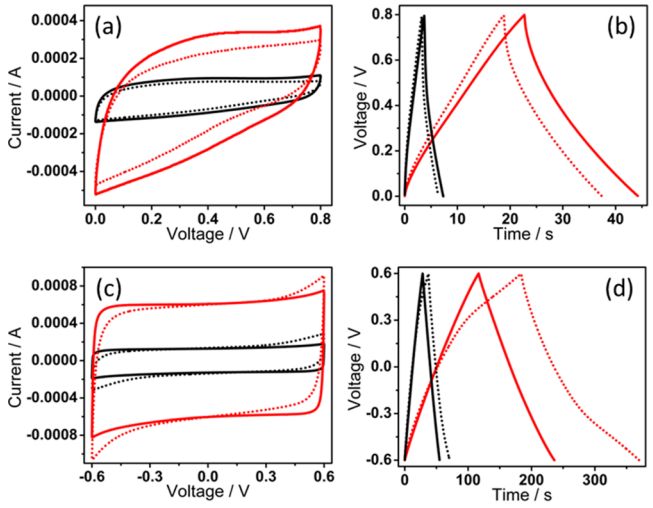

Figure 3. Electrochemical performances of solid-state supercapacitors: (a) CVs of MnO_2 nanosheets under 0 (solid lines) and 20% strain (dotted lines). (b) CDs of MnO_2 nanosheets under 0 (solid lines) and 20% strain (dotted lines). (c) CVs of PPy films under 0 (solid lines) and 20% strain (dotted lines). (d) CDs of PPy films under 0 (solid lines) and 20% strain (dotted lines).

associated with dictation. The two close peaks at 1058 and 1082 cm^{-1} (peak e and f) correspond to symmetrical C–H in-plane bending and N–H in-plane deformation. The peaks at 1250 and 1333 cm^{-1} (peak g and h) are attributed to the antisymmetrical C–H in-plane bending and antisymmetrical in-ring C–N stretching, respectively. C–C and C–N stretching are reflected at both 1381 and 1496 cm^{-1} (peak i and j). The peak at 1580 cm^{-1} (peak k) is an overlap of C–C in-ring and C–C inter-ring stretching resulting from radical cation and dictation.[33]

The electrochemical measurements of solid-state supercapacitors are conducted at room temperature, under both relaxed and stretched states (20% strain). For an MnO_2 nanosheet-based supercapacitor, the poor electrical conductivity (10^{-5} – 10^{-6} S/cm)[30] and corrosion resistance[17,34] are believed to account for the obtained nonrectangular shape of CVs. In contrast, the PPy film-based stretchable supercapacitor exhibits the good rectangular shape of CVs and the isosceles triangle shape of CDs. These should arise from the high electrical conductivity and great corrosion resistance of the electrochemically deposited PPy film. Interestingly enough, the performance of the two supercapacitors exhibit totally different responses to strain. For the MnO_2 nanosheet-based supercapacitor, as demonstrated in Figure 3a, areas of CVs under the stretched states decrease remarkably, and consistently, discharge times decrease as well (Figure 3b). Conversely, for the PPy film-based supercapacitor, areas of CVs and discharge times increase under the applied stretch (Figure 3c,d). These observations are observed and confirmed by more CVs and CDs shown in Figure S3 (Supporting Information).[24] In addition, it should be noted that compared with the MnO_2 nanosheet supercapacitor, these electrochemical curves of PPy film-supercapacitors are more sensitive to strain, as revealed by their distorted shapes. It should be noted that the variation of electrochemical curves is related to the increase of intrinsic charge transfer resistance (150% incease) instead of morphology change exhibited in Figure 4. These observations clearly demonstrate that with the same substrate and electrolyte

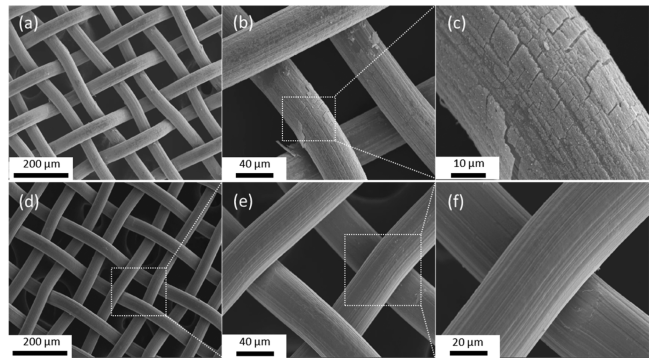

Figure 4. SEM images of the fabricated electrodes: (a–c) MnO_2 nanosheet electrode after being deformed about four stretching–releasing cycles. (d–f) PPy film electrode after being deformed about four stretching–releasing cycles.

materials but different electrochemically active materials, the tolerance to stretch-induced performance degradation could be totally different.

To understand the mechanism behind this, detailed SEM investigations were carried out, and the results are shown in Figure 4. It is observed that after being deformed about four cycles, there are many cracks on the electrodeposited MnO_2 nanosheets layer, especially at areas of cross-intersections where even some MnO_2 nanosheets fall off the substrate (Figure 4a–c). This is believed to greatly hamper the electronic transportation and ionic diffusion. By remarkable constrast, the continuous film of PPy remains well-intergrated without any visible cracks (Figure 4d–f). In addition, the rough surface of the deposited PPy film (Figure 2f) may be expanded and provide a larger electrochemically effective areas upon stretch, which contributes to the capacitance enhancement as observed.

EIS are also studied to explain the difference (Figure 5a–c). The charge transfer resistance of a PPy film is approximately 0.3

DOI: 10.1021/am507588p
ACS Appl. Mater. Interfaces 2015, 7, 2569–2574

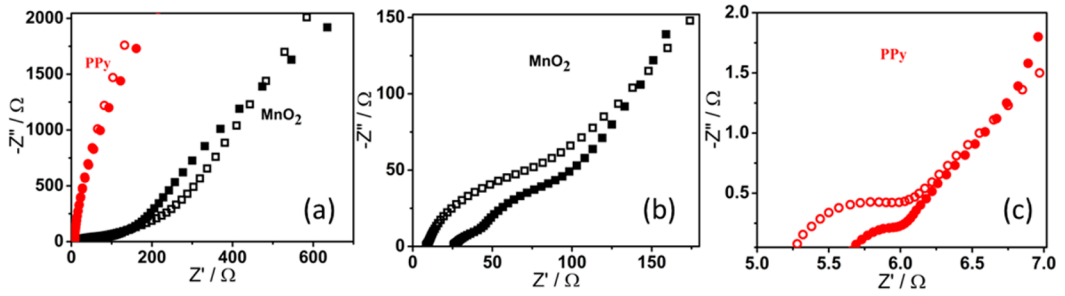

Figure 5. Electrochemical impedance spectra of solid-state supercapacitors: (a) Nyquist plots of MnO_2 nanosheets and PPy film under 0 (solid) and 20% strain (hollow). (b) A zoomed-out image of the MnO_2 nanosheets Nyquist plot under 0 (solid) and 20% strain (hollow). (c) A zoomed-out image of the PPy film Nyquist plot under 0 (solid) and 20% strain (hollow).

Ω, while that of MnO_2 nanosheets is about 75 Ω under 0 strain. The system resistance of the PPy film (5.7 Ω) is also lower than that of MnO_2 nanosheets (26 Ω), suggesting much higher ionic and electronic conductivities of PPy than those of MnO_2. Compared to the case of 0 strain, the charge transfer resistance of PPy film under 20% strain increases to 0.75 Ω, and that of MnO_2 nanosheets is around 90 Ω. This substantiates the speculation from aforementioned SEMs that cracks impede the electronic transportation and ionic diffusion of MnO_2 nanosheets under stretch. The system resistance of PPy film and MnO_2 nanosheets under 20% strain decrease to 5.25 Ω and 9 Ω, respectively. This is likely to arise from the improvement of electrical contacts between active materials upon stretch.[35]

Keeping in mind that metal oxides are a big category of electrochemically active materials for supercapacitors and their intrinsic rigid structures, it is primarily important to solve the mismatch problem to prevent strain-induced performance degradation of strecthable devices. A reasonable idea is to combine the conducting polymer, which is intrisically flexible, with metal oxides together to enhance the systematic tolerance. As a trial, an electrode structure fabricated by MnO_2 coated on the conductive mesh followed by a certain amount of PPy deposition was designed. Figure 6a and b show clearly that

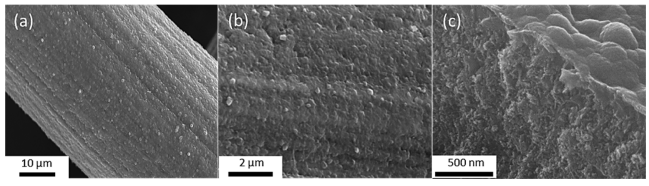

Figure 6. Characterization of PPy-penetrated MnO_2 electrode: (a,b) top views of the electrode surface. (c) Side view of the PPy-penetrated MnO_2 composite electrode structure.

most of the flower-like MnO_2 nanosheets are covered by PPy to form a composite structure, making the surface smoother than that of pure MnO_2 nanosheets, while rougher than that of pure PPy shown in Figures 2c and f. It should be noted that PPy film does not only cover the top surface of the MnO_2 layer but also penetrate into the whole thickness of the pores among MnO_2 nanosheets as shown in Figure 6c. The pores among flower-like MnO_2 nanosheets allow the formation of a uniform PPy-penetrated MnO_2 composite layer. C elemental mapping in the whole PPy-MnO_2 layer (Figure S5a,b, Supporting Information) as well as the porous cross-section of MnO_2 (Figure S5c, Supporting Information) further confirm the penetration of PPy.

PPy penetration remarkably enhances the tolerance to performance degradation of the MnO_2 nanosheet-based stretchable supercapacitors. As shown in Figure 7a and b,

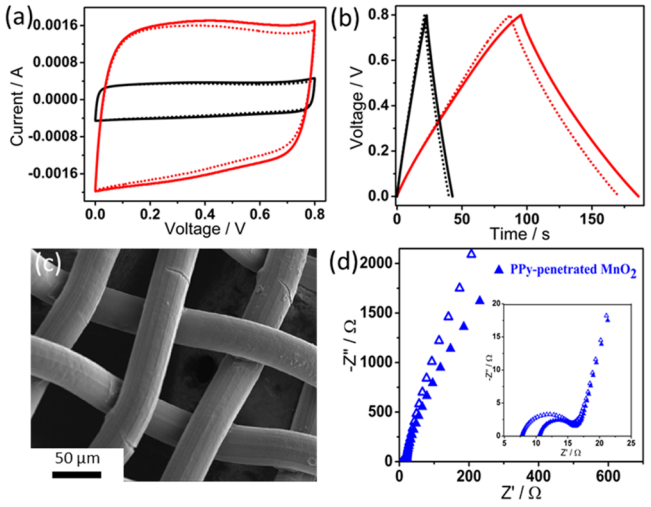

Figure 7. Electrochemical performances and characterization of the PPy-penetrated MnO_2 electrode: (a) CVs under 0 (solid lines) and 20% strain (dotted lines). (b) CDs under 0 (solid lines) and 20% strain (dotted lines). (c) SEM image of the electrode after being deformed around four stretching−releasing cycles. (d) Nyquist plot under 0 (solid) and 20% strain (hollow). The inset is a zoomed out image of the Nyquist plot showing a semicircle.

areas of CVs and discharge times decrease only a bit under stretch. Moreover, shapes of both CVs and CDs are greatly improved. These improvements arise from the flexible and conductive PPy incorporated serving as a stress buffer, which is further confirmed by the SEM image (Figure 7c). Only a few cracks appear on the PPy-penetrated MnO_2, which are not as thorough as those on pure MnO_2 nanosheets. More importantly, the loss of contact with the substrate shown in Figure 4a−c is not observed at all. It should be noted that although only about 4 stretching−releasing cycles were applied in Figures 4 and 7, the morphologies/structures of MnO_2, PPy, and PPy-penetrated MnO_2 that underwent both 1 cycle and 60 cycles (Figure S6, Supporting Information) are all highly consistent with these under 4 cycles. Under all these different loading cycles, MnO_2 breaks into small pieces, and some even fall off from the substrate. In contrast, there are no visible cracks on PPy. For the PPy-penetrated MnO_2, a few incomplete cracks can be observed. The EIS result can also explain this improvement (Figure 7d). The charge transfer resistance is 6

DOI: 10.1021/am507588p
ACS Appl. Mater. Interfaces 2015, 7, 2569−2574

Ω, being much lower than that of MnO_2 nanosheets (75 Ω) under 0 strain. The system resistance (11 Ω) is also lower than that of MnO_2 nanosheets (26 Ω), indicating that the penetration of PPy improves ionic and electronic conductivity effectively. Compared to the case of 0 strain, the charge transfer resistance under 20% strain slightly increases to 11 Ω. The system resistance under 20% strain decreases to 6 Ω, again being much lower than that of MnO_2 nanosheets (9 Ω). These resistance data are summarized in Table 1.

Table 1. Summary of System Resistances (R_s) and Charge Transfer Resistances (R_{ct}) of MnO_2 Nanosheets, PPy Film and PPy-Penetrated MnO_2 Solid State Supercapacitors

	R_s (Ω)		R_{ct} (Ω)	
	0 strain	20% strain	0 strain	20% strain
MnO_2	26	9	75	90
PPy	5.7	5.25	0.3	0.75
PPy-penetrated MnO_2	11	6	6	11

To further demonstrate the advantage of PPy penertration for the performance perservation of the fabricated stretchable supercapacitors, specific capacitances as functions of scan rates for all three supercapacitors mentioned above under 0 and 20% strain are shown in Figure 8a. The specific capacitance (C_s) was

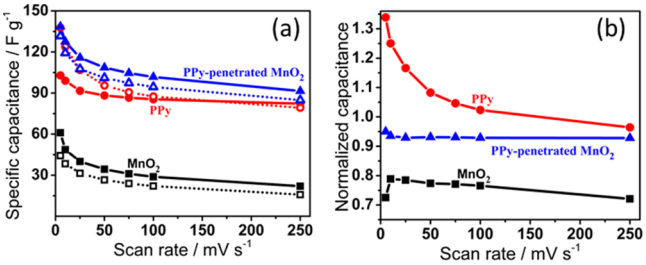

Figure 8. Electrochemical performances of solid-state supercapacitors: (a) specific capacitances as functions of scan rates under 0 (solid lines) and 20% strain (dotted lines). (b) Normalized specific capacitances as functions of scan rates.

calculated using the voltammetric charge integrated from CV curves according to the formula

$$C_s = \frac{Q}{Vm} = \frac{1}{Vvm}\int_{V_-}^{V_+}(V)dV \quad (1)$$

where Q is the total charge obtained by integrating the positive and negative sweeps of the CV curve, V is the voltage range ($V = V_+ - V_-$), v is the scan rate, and m is the mass of active materials per electrode. PPy-penetrated MnO_2 exhibits the highest capacitances, while the relatively low capacitances of MnO_2 are likely attributed to some acid corrosion.[17,18] Tao et al.[17] discussed in detail the serious corrosion of MnO_2 in aqueous H_3PO_4. A certain amount of PPy electrodeposited on MnO_2 can provide protection against acidic corrosion. Under the strain of 20%, capacitances of both PPy-penetrated MnO_2 and MnO_2 decrease at all scan rates, compared to those under the 0 strain. Capacitance enhancement is observed for the PPy electrode at scan rates studied in this work. The normalized capacitances (obtained by dividing the capacitance under the 20% strain by the one under the 0 strain at the same scan rate) clearly reflect the change of capacitance induced by stretch (Figure 8b). Both the PPy film and MnO_2 nanosheets show a decreased normalized capacitances with the increase of scan rate. The number decreases from over 1.3 to 0.96 for the PPy film and is always lower than 0.8 at all scan rates for MnO_2 nanosheets. However, the PPy-penetrated MnO_2 electrode keeps a stable normalized number, slightly fluctuating between 0.93 to 0.95, which is much better than the pure MnO_2 nanosheets electrode, indicating an effectively enhanced tolerance to the stretch-induced performance degradation of MnO_2. This enhancement should be attributed to improved materials matching between the substrate and electrochemically active materials upon stretch.

4. CONCLUSIONS

The electrodes of stretchable supercapacitors usually consist of electrochemically active materials such as carbon, metal oxides, and conducting polymers, as well as the stretchable conducting substrate. Here, we present a systematic study on the influence of materials matching on strain-induced performance degradation, as well as how to enhance the tolerance to the degradation of metal oxides. It is revealed that the performance of MnO_2 nanosheet electrodes degrades remarkably under stretch, while for PPy film electrodes, the performance can be well preserved and even enhanced with the applied strain. These are attributed to their intrinsic structural properties, different morphology variation, and corresponding impedance variation upon stretch. Finally, it is demonstrated that the electrode structure of PPy-penetrated MnO_2 can achieve remarkably enhanced tolerance toward the severe stretch-induced performance degradation in comparison with pure MnO_2 nanosheets as electrodes. Our study indicates that although metal oxides are usually utilized as high performance electrode materials of stretchable supercapacitors, it is actually very imperative to introduce conducting polymers to achieve excellent tolerance to strain-induced performance degradation and to guarantee long-term stability of the devices. Our study provides an important guideline for materials selection and matching to design and optimize stretchable electronic devices.

■ ASSOCIATED CONTENT

Supporting Information

Chronoamperometry during PPy electrodeposition at different potentials; SEM images of the PPy electrodeposited at different potentials; the PPy-penetrated MnO_2 electrode; and the cross-section of the MnO_2 as well as MnO_2, PPy, and PPy-penetrated MnO_2 electrodes after being deformed 1 and 60 stretching–releasing cycles; C elemental mapping of the PPy-penetrated MnO_2 electrode; TEM EDX of the electrodeposited MnO_2; and electrochemical performances of MnO_2, PPy, and PPy-penetrated MnO_2 supercapacitors. This material is available free of charge via the Internet at http://pubs.acs.org.

■ AUTHOR INFORMATION

Corresponding Author

*Tel: +852-34427891. E-mail: cy.zhi@cityu.edu.hk.

Notes

The authors declare no competing financial interest.

■ ACKNOWLEDGMENTS

This research was supported by the Early Career Scheme of the Research Grants Council of Hong Kong SAR, China, under Project Number CityU 9041977, the Science Technology and Innovation Committee of Shenzhen Municipality (Grant

DOI: 10.1021/am507588p
ACS Appl. Mater. Interfaces 2015, 7, 2569–2574

Number JCYJ20130401145617276), and a grant from the City University of Hong Kong. We thank T. F. Hung, T. C. Lau, J. P. Wang, and W. Chen for their experimental support.

REFERENCES

(1) Bowden, N.; Brittain, S.; Evans, A. G.; Hutchinson, J. W.; Whitesides, G. M. Spontaneous Formation of Ordered Structures in Thin Films of Metals Supported on an Elastomeric Polymer. *Nature* **1998**, *393*, 146−149.

(2) Lacour, S. P.; Wagner, S.; Huang, Z. Y.; Suo, Z. Stretchable Gold Conductors on Elastomeric Substrates. *Appl. Phys. Lett.* **2003**, *82*, 2404−2406.

(3) Filiatrault, H. L.; Porteous, G. C.; Carmichael, R. S.; Davidson, G. J. E.; Carmichael, T. B. Stretchable Light-Emitting Electrochemical Cells Using an Elastomeric Emissive Material. *Adv. Mater.* **2012**, *24*, 2673−2678.

(4) Lipomi, D. J.; Vosgueritchian, M.; Tee, B. C. K.; Hellstrom, S. L.; Lee, J. A.; Fox, C. H.; Bao, Z. N. Skin-Like Pressure and Strain Sensors Based on Transparent Elastic Films of Carbon Nanotubes. *Nat. Nanotechnol.* **2011**, *6*, 788−792.

(5) Li, X.; Gu, T. L.; Wei, B. Q. Dynamic and Galvanic Stability of Stretchable Supercapacitors. *Nano Lett.* **2012**, *12*, 6366−6371.

(6) Park, S.; Jayaraman, S. Smart Textiles: Wearable Electronic Systems. *MRS Bull.* **2003**, *28*, 585−591.

(7) Kim, D. H.; Lu, N. S.; Ma, R.; Kim, Y. S.; Kim, R. H.; Wang, S. D.; Wu, J.; Won, S. M.; Tao, H.; Islam, A.; Yu, K. J.; Kim, T. I.; Chowdhury, R.; Ying, M.; Xu, L. Z.; Li, M.; Chung, H. J.; Keum, H.; McCormick, M.; Liu, P.; Zhang, Y. W.; Omenetto, F. G.; Huang, Y. G.; Coleman, T.; Rogers, J. A. Epidermal Electronics. *Science* **2011**, *333*, 838−843.

(8) Song, Y. M.; Xie, Y. Z.; Malyarchuk, V.; Xiao, J. L.; Jung, I.; Choi, K. J.; Liu, Z. J.; Park, H.; Lu, C. F.; Kim, R. H.; Li, R.; Crozier, K. B.; Huang, Y. G.; Rogers, J. A. Digital Cameras with Designs Inspired by the Arthropod Eye. *Nature* **2013**, *497*, 95−99.

(9) Ahn, J. H.; Je, J. H. Stretchable Electronics: Materials, Architectures and Integrations. *J. Phys. D: Appl. Phys.* **2012**, *45*, 1−14.

(10) Kaltenbrunner, M.; Kettlgruber, G.; Siket, C.; Schwodiauer, R.; Bauer, S. Arrays of Ultracompliant Electrochemical Dry Gel Cells for Stretchable Electronics. *Adv. Mater.* **2010**, *22*, 2065−2067.

(11) Lipomi, D. J.; Tee, B. C. K.; Vosgueritchian, M.; Bao, Z. N. Stretchable Organic Solar Cells. *Adv. Mater.* **2011**, *23*, 1771−1775.

(12) Wang, C. Y.; Zheng, W.; Yue, Z. L.; Too, C. O.; Wallace, G. G. Buckled, Stretchable Polypyrrole Electrodes for Battery Applications. *Adv. Mater.* **2011**, *23*, 3580−3584.

(13) Jost, K.; Stenger, D.; Perez, C. R.; McDonough, J. K.; Lian, K.; Gogotsi, Y.; Dion, G. Knitted and Screen Printed Carbon-Fiber Supercapacitors for Applications in Wearable Electronics. *Energy Environ. Sci.* **2013**, *6*, 2698−2705.

(14) Lipomi, D. J.; Chong, H.; Vosgueritchian, M.; Mei, J. G.; Bao, Z. A. Toward Mechanically Robust and Intrinsically Stretchable Organic Solar Cells: Evolution of Photovoltaic Properties with Tensile Strain. *Sol. Energy Mater. Sol. Cells* **2012**, *107*, 355−365.

(15) Xie, K.; Wei, B. Materials and Structures for Stretchable Energy Storage and Conversion Devices. *Adv. Mater.* **2014**, 3592−3617.

(16) Wang, X. F.; Lu, X. H.; Liu, B.; Chen, D.; Tong, Y. X.; Shen, G. Z. Flexible Energy-Storage Devices: Design Consideration and Recent Progress. *Adv. Mater.* **2014**, *26*, 4763−4782.

(17) Tao, J. Y.; Liu, N. S.; Ma, W. Z.; Ding, L. W.; Li, L. Y.; Su, J.; Gao, Y. H. Solid-State High Performance Flexible Supercapacitors Based on Polypyrrole-MnO_2-Carbon Fiber Hybrid Structure. *Sci. Rep.* **2013**, *3*, 1−7.

(18) Tao, J. Y.; Liu, N. S.; Li, L. Y.; Gao, Y. H. Hierarchical Nanostructures of Polypyrrole@MnO_2 Composite Electrodes for High Performance Solid-State Asymmetric Supercapacitors. *Nanoscale* **2014**, *6*, 2922−2928.

(19) Simon, P.; Gogotsi, Y. Materials for Electrochemical Capacitors. *Nat. Mater.* **2008**, *7*, 845−854.

(20) Conway, B. E. *Electrochemical Supercapacitors: Scientific Fundamentals and Technological Applications*; Springer: New York, 1999.

(21) Wang, X. F.; Liu, B.; Liu, R.; Wang, Q. F.; Hou, X. J.; Chen, D.; Wang, R. M.; Shen, G. Z. Fiber-Based Flexible All-Solid-State Asymmetric Supercapacitors for Integrated Photodetecting System. *Angew. Chem., Int. Ed.* **2014**, *53*, 1849−1853.

(22) Wang, X. B.; Zhang, Y. J.; Zhi, C. Y.; Wang, X.; Tang, D. M.; Xu, Y. B.; Weng, Q. H.; Jiang, X. F.; Mitome, M.; Golberg, D.; Bando, Y. Three-Dimensional Strutted Graphene Grown by Substrate-Free Sugar Blowing for High-Power-Density Supercapacitors. *Nat. Commun.* **2013**, *4*, 1−8.

(23) Yuan, L. Y.; Xiao, X.; Ding, T. P.; Zhong, J. W.; Zhang, X. H.; Shen, Y.; Hu, B.; Huang, Y. H.; Zhou, J.; Wang, Z. L. Paper-Based Supercapacitors for Self-Powered Nanosystems. *Angew. Chem., Int. Ed.* **2012**, *51*, 4934−4938.

(24) Yue, B. B.; Wang, C. Y.; Ding, X.; Wallace, G. G. Polypyrrole Coated Nylon Lycra Fabric as Stretchable Electrode for Supercapacitor Applications. *Electrochim. Acta* **2012**, *68*, 18−24.

(25) Liu, Z.; Xu, J.; Chen, D.; Shen, G. Flexible Electronics Based on Inorganic Nanowires. *Chem. Soc. Rev.* **2014**, *44*, 161−192.

(26) Liu, B.; Liu, B. Y.; Wang, Q. F.; Wang, X. F.; Xiang, Q. Y.; Chen, D.; Shen, G. Z. New Energy Storage Option: Toward $ZnCo_2O_4$ Nanorods/Nickel Foam Architectures for High-Performance Supercapacitors. *ACS Appl. Mater. Interfaces* **2013**, *5*, 10011−10017.

(27) Xu, J.; Wang, Q. F.; Wang, X. W.; Xiang, Q. Y.; Hang, B.; Chen, D.; Shen, G. Z. Flexible Asymmetric Supercapacitors Based upon Co_9S_8 Nanorod//Co_3O_4@RuO_2 Nanosheet Arrays on Carbon Cloth. *ACS Nano* **2013**, *7*, 5453−5462.

(28) Liu, D. Q.; Wang, X.; Wang, X. B.; Tian, W.; Liu, J. W.; Zhi, C. Y.; He, D. Y.; Bando, Y.; Golberg, D. Ultrathin Nanoporous Fe_3O_4-Carbon Nanosheets with Enhanced Supercapacitor Performance. *J. Mater. Chem. A* **2013**, *1*, 1952−1955.

(29) Zhao, L.; Yu, J.; Li, W. J.; Wang, S. G.; Dai, C. L.; Wu, J. W.; Bai, X. D.; Zhi, C. Y. Honeycomb Porous MnO_2 Nanofibers Assembled from Radially Grown Nanosheets for Aqueous Supercapacitors with High Working Voltage and Energy Density. *Nano Energy* **2014**, *4*, 39−48.

(30) Chen, W.; Rakhi, R. B.; Hu, L. B.; Xie, X.; Cui, Y.; Alshareef, H. N. High-Performance Nanostructured Supercapacitors on a Sponge. *Nano Lett.* **2011**, *11*, 5165−5172.

(31) Tao, T.; Glushenkov, A. M.; Liu, H. W.; Liu, Z. W.; Dai, X. J. J.; Chen, H.; Ringer, S. P.; Chen, Y. Ilmenite $FeTiO_3$ Nanoflowers and Their Pseudocapacitance. *J. Phys. Chem. C* **2011**, *115*, 17297−17302.

(32) Perera, S. D.; Rudolph, M.; Mariano, R. G.; Nijem, N.; Ferraris, J. P.; Chabal, Y. J.; Balkus, K. J. Manganese Oxide Nanorod-Graphene/Vanadium Oxide Nanowire-Graphene Binder-Free Paper Electrodes for Metal Oxide Hybrid Supercapacitors. *Nano Energy* **2013**, *2*, 966−975.

(33) Wang, J.; Xu, Y. L.; Yan, F.; Zhu, J. B.; Wang, J. P. Template-Free Prepared Micro/Nanostructured Polypyrrole with Ultrafast Charging/Discharging Rate and Long Cycle Life. *J. Power Sources* **2011**, *196*, 2373−2379.

(34) Liu, N. S.; Ma, W. Z.; Tao, J. Y.; Zhang, X. H.; Su, J.; Li, L. Y.; Yang, C. X.; Gao, Y. H.; Golberg, D.; Bando, Y. Cable-Type Supercapacitors of Three-Dimensional Cotton Thread Based Multi-Grade Nanostructures for Wearable Energy Storage. *Adv. Mater.* **2013**, *25*, 4925−4931.

(35) Hu, L. B.; Pasta, M.; La Mantia, F.; Cui, L. F.; Jeong, S.; Deshazer, H. D.; Choi, J. W.; Han, S. M.; Cui, Y. Stretchable, Porous, and Conductive Energy Textiles. *Nano Lett.* **2010**, *10*, 708−714.

DOI: 10.1021/am507588p
ACS Appl. Mater. Interfaces 2015, 7, 2569−2574